Asian Journal of Chemistry; Vol. 28, No. 1 (2016), 86-90

ASIAN JOURNAL OF CHEMISTRY

http://dx.doi.org/10.14233/ajchem.2016.19247

Hydrothermally Synthesis and Characterization of Lanthanide Coordination Polymers with $(4^2.6^2.8^2)(4^3.6^3)_2(4^6.6^7.8^2)(4^8.6^7)$ Topology $\{[Ln_2(1,4\text{-pda})_3(H_2O)]\cdot 2H_2O\}_n$ (Ln = Pr, Nd, Dy)

MEI-LI ZHANG*, NA GAO, LOU-JUN GAO, XU-HUA HAN and XIAO-LI CHEN

Department of Chemistry and Chemical Engineering, Yan'an University, Shaanxi 716000, P.R. China

*Corresponding author: Tel: +86 911 2332037; E-mail: ydzml2332041@163.com

Received: 14 April 2015; *Accepted*: 2 June 2015; *Published online*: 5 October 2015; AJC-17551

Three 3D lanthanide coordination polymers $\{[Ln_2(1,4\text{-pda})_3(H_2O)]\cdot 2H_2O\}_n$ (1,4-pda = 1,4-phenylenediacetic acid, Ln = Pr for **1**, Nd for **2** and Dy for **3**) have been hydrothermally synthesized and characterized by elemental analysis, IR spectroscopy, thermogravimetric analyses and single-crystal X-ray diffraction techniques. The structure indicates that three complexes have similar structures and belong to monoclinic crystal system, $P2_1/c$ space group. In which, *trans-bis*(μ_2-η^2:η^1) and *trans-bis*(μ_2-η^1:η^1) 1,4-pda^{2-} anions link the Ln(III) center to generate a 2D network, furthermore, the dimensionality is extended to a (4,6)-connected 3D architecture with a Schläfli symbol of $(4^2.6^2.8^2)(4^3.6^3)_2(4^6.67.8^2)(4^8.6^7)$ through same coordination mode 1,4-pda^{2-} anions linking. In additional, photoluminescence properties of three complexes have also been studied. (CCDC 1009612 for **1**, 1009613 for **2** and 1009614 for **3**).

Keywords: Lanthanide coordination polymers, Crystal structure, Luminescence.

INTRODUCTION

The rational design and controlled synthesis of metal-organic frameworks (MOFs), also known as coordination polymers, has become an exciting field owing to their unique structural characteristics and intriguing framework diversities [1,2] and potential application in gas storage, catalysis, ion exchange, magnetism, molecular recognition and separation, *etc.* [3-7]. Among them, lanthanide-metal-organic frameworks (LMOFs) are particularly desirable for their luminescence, electronic, optical and chemical characteristics arising from the 4*f* electronic shells. The aromatic N- and O-containing polycarboxylic ligands are often regarded as an effective strategy for the construction of LMOFs [8,9]. In these kinds of ligands, rigid polycarboxylic acids are frequently used to link lanthanide ions or lanthanide clusters [10,11]. In contrast, far less common has been focused on the investigation of flexible polycarboxylic acid ligands [12,13]. This is probably due to the flexibility of the ligand skeletons, which makes it more difficult to control their structures in the final coordination networks. However, as for the flexible multifunctional ligands, the backbone flexibility and conformation changeability afford their versatile bridging modes and make the structures of their complexes more diversiform and more difficult to predict [14,15].

With the above in mind, we would like to synthesize and explore new LMOFs with flexible 1,4-phenylenediacetate (1,4-pda) and only five lanthanide examples of 1,4-pda ligand have been reported with formula $\{[Ln_2(1,4\text{-pda})_3(H_2O)]\cdot 2H_2O\}_n$ (Ln= La, Eu, Gd, Tb, Er) [16,17]. Herein, we report three new lanthanide coordination polymers with 1,4-pda, $\{[Ln_2(1,4\text{-pda})_3(H_2O)]\cdot 2H_2O\}_n$ (Ln = Pr, Nd, Dy). Three complexes have the unusual 3D architectures.

EXPERIMENTAL

All chemicals and reagents were used as received from commercial sources without further purification. All reactions were carried out under hydrothermal conditions. Elemental analyses (C, H, N) were determined with a Elementar Vario EL III elemental analyzer; IR spectra were recorded as KBr pellets on a Bruker EQUINOX55 spectrophotometer in the 4000-400 cm^{-1} region. Fluorescence spectra were performed on a Hitachi F-4500 fluorescence spectrophotometer at room temperature. Thermogravimetric analyses (TGA) was performed on a Universal V2.6 DTA Instruments.

Syntheses: $\{[Pr_2(1,4\text{-pda})_3(H_2O)]\cdot 2H_2O\}_n$ (**1**) was synthesized from the reaction mixture of $Pr(NO_3)_3$ (0.1 mmol), 1,4-H_2pda (0.1 mmol), sodium acetate (0.2 mmol) and water (12 mL) in a 25 mL Parr Teflon-lined stainless steel vessel under autogenous pressure at 140 °C for 96 h and then cooled to room temperature at a rate of 5 °C/h. Green block crystals of **1** were obtained (yield 45 % based on 1,4-H_2pda). Anal. calcd. for $C_{30}H_{30}O_{15}Pr_2$ (912.36): C, 39.46 %, H, 3.29 %; Found: C,

39.28 %, H, 3.15 %. IR data (KBr, ν_{max}, cm^{-1}): 3437 (br), 2966(w), 1587(s), 1427(s), 1280(s), 1201(m), 1026(w), 950(m), 867(w), 719(s), 615(w).

{[Nd_2(1,4-pda)$_3$(H_2O)]·2H_2O}$_n$ (2): A synthetic procedure similar to that for **1** was used except that $Pr(NO_3)_3$ was replaced by $Nd(NO_3)_3$ for **2**, with different yield(43 % for **2**, based on 1,4-H_2pda). Anal. calcd. for $C_{30}H_{30}O_{15}Nd_2$(919.02): C, 39.17 %, H, 3.26 %; Found: C, 39.75 %, H, 3.49 %. IR data (KBr, ν_{max}, cm^{-1}): 3452 (br), 2960(w), 1546(s), 1398(s), 1280(s), 1203(m), 1159(m), 952(m), 719 (s).

{[Dy_2(1,4-pda)$_3$(H_2O)]·2H_2O}$_n$ (3): A synthetic procedure similar to that for **1** was used except that $Pr(NO_3)_3$ was replaced by $Dy(NO_3)_3$ for **3**, with different yield (48 % for **3**, based on 1,4-H_2pda). Anal. calcd. for $C_{30}H_{30}O_{15}Dy_2$(955.54): C, 37.68 %, H, 3.14 %; Found: C, 36.75 %, H, 3.29 %. IR data (KBr, ν_{max}, cm^{-1}): 3334 (br), 2953(w), 1672(s), 1583(s), 1523(s), 1454(s), 1317(m), 1143(m), 927(w), 788(w), 729 (s).

X-ray crystallography: Diffraction intensities for the complexes **1**, **2** and **3** were collected at 296 K on a Bruker SMART 1000 CCD diffractometer employing graphite-monochromated Mo-K_α radiation (λ = 0.071073 nm). A semiempirical absorption correction was applied using the SADABS program [18]. The structure was solved by direct methods and refined by full-matrix least-squares on F^2 using the SHELXS 97 and SHELXL 97 programs, respectively [19,20]. Non-hydrogen atoms were refined anisotropically and hydrogen atoms were placed in geometrically calculated positions. The crystallographic data for complexes are listed in Table-1 and selected bond lengths and angles are listed in Table-2. (CCDC 1009612 for **1**, 1009613 for **2** and 1009614 for **3**).

RESULTS AND DISCUSSION

Description of crystal structure: Single-crystal X-ray diffraction analysis reveals that {[Ln_2(1,4-pda)$_3$(H_2O)]·2H_2O}$_n$ (Ln = Pr for **1**, Nd for **2** and Dy for **3**) complexes have similar structures and belong to monoclinic crystal system, $P2_1/c$ space group. Therefore, only the structure of **1** will be discussed in detail as a representative. In **1**, there is two crystallographically independent Pr^{3+} ions with the 9-coordinated distorted single-capped anti-square prism geometries (Fig. 1). Pr1 is coordinated by six O atoms (O(1), O(2), O(3)A, O(5), O(7)B and O(8)B) of four μ_2–η^2:η^1 carboxylates, two O atoms (O(11) and O(9)) of two *bis*(monodentate) bridging carboxylates and one O atom (O(13)) of one water ligand. The nine oxygen atoms coordinated to Pr2 are from one *bis*(monodentate) bridging carboxylate group (O(10)), eight O atoms (O(2), O(3)F, O(4)F, O(5), O(6), O(8)D, O(11)E and O(12)E) of μ_2–η^2:η^1 mode chelating carboxyl groups. The Pr–O distances range from 2.364(3) to 2.679(3) Å and the O–Pr–O angles range from 49.34(9) to 166.82(12)°, which are similar to those found in other related examples [14].

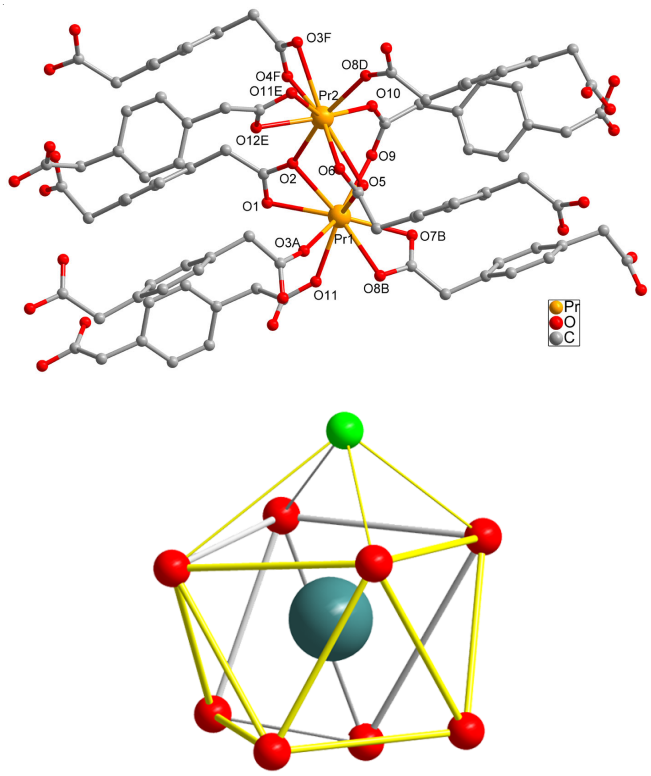

Fig. 1. Coordination environments of Pr atom in complex **1**. All hydrogen atoms are omitted for clarity. Symmetry code: A -x,y-1/2,-z+1/2; B -x+1,y+1/2,-z+1/2; D -x+1,-y,-z+1; E x,-y+1/2,z+1/2; F -x,-y+1,-z+1

TABLE-1
CRYSTALLOGRAPHIC DATE FOR COMPLEXES **1**, **2** AND **3**

Complex	Complex **1**	Complex **2**	Complex **3**
Empirical formula	$C_{30}H_{30}O_{15}Pr_2$	$C_{30}H_{30}O_{15}Nd_2$	$C_{30}H_{30}O_{15}Dy_2$
Formula weight	912.36	919.02	955.54
Crystal system	Monoclinic	Monoclinic	Monoclinic
Space group	$P2_1/c$	$P2_1/c$	$P2_1/c$
a (nm)	2.1947(3)	2.1986(3)	2.17489(11)
b (nm)	1.01300(11)	1.01561(14)	1.00499(5)
c (nm)	1.41241(16)	1.41058(19)	1.39931(7)
β (°)	91.528(2)	91.588(2)	91.6610(10)
V (nm^3)	3.1390(6)	3.1485(7)	3.0572(3)
Z	4	4	4
Dc (mg m^{-3})	1.931	1.939	2.076
Absorption coefficient (mm^{-1})	3.141	3.335	4.926
F (000)	1792	1800	1848
T (K)	296(2)	296(2)	296(2)
R_{int}	0.0233	0.0239	0.0154
Goodness-of-fit on F^2	1.079	1.041	0.982
R_1^a / wR_2^b [I >2σ(I)]	0.0282 / 0.0669	0.0326 / 0.0828	0.0159 / 0.0525
R_1^a / wR_2^b (All data)	0.0302 / 0.0679	0.0390 / 0.0867	0.0197 / 0.0615

TABLE-2
SELECTED BOND LENGTH (nm) AND ANGLE (°) FOR COMPLEXES **1**, **2** and **3**

Complex **1**					
Pr(1)-O(9)	2.433(3)	Pr(1)-O(7)#2	2.554(3)	Pr(2)-O(12)#5	2.442(3)
Pr(1)-O(13)	2.436(4)	Pr(1)-O(1)	2.565(3)	Pr(2)-O(4)#6	2.495(3)
Pr(1)-O(11)	2.461 (3)	Pr(1)-O(8)#2	2.611(3)	Pr(2)-O(6)	2.498(3)
Pr(1)-O(3)#1	2.481(3)	Pr(2)-O(10)	2.364(3)	Pr(2)-O(11)#5	2.668(3)
Pr(1)-O(5)	2.503(3)	Pr(2)-O(2)	2.406(3)	Pr(2)-O(3)#6	2.674(3)
Pr(1)-O(2)	2.531(3)	Pr(2)-O(8)#4	2.412(3)	Pr(2)-O(5)	2.679(3)
O(9)-Pr(1)-O(13)	71.88(13)	O(11)-Pr(1)-O(2)	121.86(10)	O(3)#1-Pr(1)-O(1)	78.76(12)
O(9)-Pr(1)-O(11)	144.73(11)	O(3)#1-Pr(1)-O(2)	77.79(11)	O(5)-Pr(1)-O(1)	115.95(10)
O(13)-Pr(1)-O(11)	73.60(12)	O(5)-Pr(1)-O(2)	67.96(10)	O(2)-Pr(1)-O(1)	50.04(9)
O(9)-Pr(1)-O(3)#1	145.79(11)	O(9)-Pr(1)-O(7)#2	75.31(11)	O(7)#2-Pr(1)-O(1)	158.00(14)
O(13)-Pr(1)-O(3)#1	139.13(13)	O(13)-Pr(1)-O(7)#2	81.66(16)	O(9)-Pr(1)-O(8)#2	121.34(10)
O(11)-Pr(1)-O(3)#1	69.24(10)	O(11)-Pr(1)-O(7)#2	92.86(11)	O(13)-Pr(1)-O(8)#2	111.58(13)
O(9)-Pr(1)-O(5)	75.48(11)	O(3)#1-Pr(1)-O(7)#2	116.12(11)	O(11)-Pr(1)-O(8)#2	66.22(9)
O(13)-Pr(1)-O(5)	146.86(12)	O(5)-Pr(1)-O(7)#2	84.81(13)	O(3)#1-Pr(1)-O(8)#2	67.80(9)
O(11)-Pr(1)-O(5)	137.42(9)	O(2)-Pr(1)-O(7)#2	145.15(12)	O(5)-Pr(1)-O(8)#2	80.86(9)
O(3)#1-Pr(1)-O(5)	73.82(10)	O(9)-Pr(1)-O(1)	101.82(12)	O(2)-Pr(1)-O(8)#2	138.78(11)
O(9)-Pr(1)-O(2)	77.02(12)	O(13)-Pr(1)-O(1)	76.81(15)	O(7)#2-Pr(1)-O(8)#2	49.46(10)
O(13)-Pr(1)-O(2)	109.23(14)	O(11)-Pr(1)-O(1)	76.89(9)	O(1)-Pr(1)-O(8)#2	136.71(10)
O(10)-Pr(2)-O(2)	87.79(12)	O(8)#4-Pr(2)-O(6)	84.07(11)	O(12)#5-Pr(2)-O(3)#6	80.08(12)
O(10)-Pr(2)-O(8)#4	80.65(12)	O(12)#5-Pr(2)-O(6)	82.01(13)	O(4)#6-Pr(2)-O(3)#6	49.34(9)
O(2)-Pr(2)-O(8)#4	166.91(10)	O(4)#6-Pr(2)-O(6)	164.12(12)	O(6)-Pr(2)-O(3)#6	134.87(10)
O(10)-Pr(2)-O(12)#5	158.55(13)	O(10)-Pr(2)-O(11)#5	145.14(10)	O(11)#5-Pr(2)-O(3)#6	63.43(9)
O(2)-Pr(2)-O(12)#5	76.61(11)	O(2)-Pr(2)-O(11)#5	126.39(10)	O(10)-Pr(2)-O(5)	73.38(11)
O(8)#4-Pr(2)-O(12)#5	116.12(10)	O(8)#4-Pr(2)-O(11)#5	65.97(9)	O(2)-Pr(2)-O(5)	66.95(9)
O(10)-Pr(2)-O(4)#6	77.17(13)	O(12)#5-Pr(2)-O(11)#5	50.28(9)	O(8)#4-Pr(2)-O(5)	103.53(9)
O(2)-Pr(2)-O(4)#6	73.69(11)	O(4)#6-Pr(2)-O(11)#5	103.79(10)	O(12)#5-Pr(2)-O(5)	112.54(11)
O(8)#4-Pr(2)-O(4)#6	109.30(10)	O(6)-Pr(2)-O(11)#5	73.25(10)	O(4)#6-Pr(2)-O(5)	130.99(9)
O(12)#5-Pr(2)-O(4)#6	84.29(13)	O(10)-Pr(2)-O(3)#6	95.55(11)	O(6)-Pr(2)-O(5)	49.42(9)
O(10)-Pr(2)-O(6)	114.45(13)	O(2)-Pr(2)-O(3)#6	119.93(10)	O(11)#5-Pr(2)-O(5)	122.67(9)
O(2)-Pr(2)-O(6)	95.26(12)	O(8)#4-Pr(2)-O(3)#6	67.73(9)	O(3)#6-Pr(2)-O(5)	167.26(9)
Complex **2**					
Nd(1)-O(12)#1	2.421(4)	Nd(1)-O(8)#3	2.550(4)	Nd(2)-O(10)	2.440(4)
Nd(1)-O(13)	2.429(5)	Nd(1)-O(2)	2.558(4)	Nd(2)-O(5)	2.485(4)
Nd(1)-O(9)	2.451(4)	Nd(1)-O(7)#3	2.605(4)	Nd(2)-O(3)#2	2.492(4)
Nd(1)-O(4)#2	2.470(4)	Nd(2)-O(11)	2.362(4)	Nd(2)-O(9)	2.664(4)
Nd(1)-O(6)#1	2.491(4)	Nd(2)-O(7)#3	2.398(4)	Nd(2)-O(4)#2	2.669(4)
Nd(1)-O(1)	2.518(4)	Nd(2)-O(1)#4	2.394(4)	Nd(2)-O(6)	2.675(4)
O(12)#1-Nd(1)-O(13)	71.42(16)	O(9)-Nd(1)-O(1)	121.99(12)	O(4)#2-Nd(1)-O(2)	79.17(18)
O(12)#1-Nd(1)-O(9)	144.13(14)	O(4)#2-Nd(1)-O(1)	77.99(13)	O(6)#1-Nd(1)-O(2)	116.12(14)
O(13)-Nd(1)-O(9)	73.40(15)	O(6)#1-Nd(1)-O(1)	67.83(12)	O(1)-Nd(1)-O(2)	50.25(13)
O(12)#1-Nd(1)-O(4)#2	146.08(14)	O(12)#1-Nd(1)-O(8)#3	75.14(15)	O(8)#3-Nd(1)-O(2)	157.6(2)
O(13)-Nd(1)-O(4)#2	139.44(17)	O(13)-Nd(1)-O(8)#3	81.2(2)	O(12)#1-Nd(1)-O(7)#3	121.56(13)
O(9)-Nd(1)-O(4)#2	69.56(13)	O(9)-Nd(1)-O(8)#3	92.88(15)	O(13)-Nd(1)-O(7)#3	111.32(17)
O(12)#1-Nd(1)-O(6)#1	75.59(14)	O(4)#2-Nd(1)-O(8)#3	116.19(14)	O(9)-Nd(1)-O(7)#3	66.24(12)
O(13)-Nd(1)-O(6)#1	146.48(16)	O(6)#1-Nd(1)-O(8)#3	84.94(17)	O(4)#2-Nd(1)-O(7)#3	67.62(12)
O(9)-Nd(1)-O(6)#1	137.95(12)	O(1)-Nd(1)-O(8)#3	145.03(15)	O(6)#1-Nd(1)-O(7)#3	81.20(12)
O(4)#2-Nd(1)-O(6)#1	73.92(13)	O(12)#1-Nd(1)-O(2)	101.57(17)	O(1)-Nd(1)-O(7)#3	138.90(13)
O(12)#1-Nd(1)-O(1)	77.04(14)	O(13)-Nd(1)-O(2)	76.8(2)	O(8)#3-Nd(1)-O(7)#3	49.73(13)
O(13)-Nd(1)-O(1)	109.38(17)	O(9)-Nd(1)-O(2)	76.77(13)	O(2)-Nd(1)-O(7)#3	136.68(15)
O(11)-Nd(2)-O(7)#3	80.53(15)	O(1)#4-Nd(2)-O(3)#2	73.78(13)	O(10)-Nd(2)-O(4)#2	80.45(15)
O(11)-Nd(2)-O(1)#4	87.54(15)	O(10)-Nd(2)-O(3)#2	84.15(17)	O(5)-Nd(2)-O(4)#2	134.69(13)
O(7)#3-Nd(2)-O(1)#4	166.46(13)	O(5)-Nd(2)-O(3)#2	164.08(16)	O(3)#2-Nd(2)-O(4)#2	49.39(12)
O(11)-Nd(2)-O(10)	158.32(17)	O(11)-Nd(2)-O(9)	144.93(13)	O(9)-Nd(2)-O(4)#2	63.51(12)
O(7)#3-Nd(2)-O(10)	116.35(13)	O(7)#3-Nd(2)-O(9)	65.97(12)	O(11)-Nd(2)-O(6)	73.46(14)
O(1)#4-Nd(2)-O(10)	76.82(14)	O(1)#4-Nd(2)-O(9)	126.83(13)	O(7)#3-Nd(2)-O(6)	103.48(12)
O(11)-Nd(2)-O(5)	114.82(16)	O(10)-Nd(2)-O(9)	50.51(13)	O(1)#4-Nd(2)-O(6)	66.66(12)
O(7)#3-Nd(2)-O(5)	83.94(14)	O(5)-Nd(2)-O(9)	73.08(12)	O(10)-Nd(2)-O(6)	112.61(15)
O(1)#4-Nd(2)-O(5)	95.41(14)	O(3)#2-Nd(2)-O(9)	103.71(13)	O(5)-Nd(2)-O(6)	49.80(12)
O(10)-Nd(2)-O(5)	81.96(17)	O(11)-Nd(2)-O(4)#2	95.04(14)	O(3)#2-Nd(2)-O(6)	130.90(12)
O(11)-Nd(2)-O(3)#2	77.04(16)	O(7)#3-Nd(2)-O(4)#2	67.54(12)	O(9)-Nd(2)-O(6)	122.88(11)
O(7)#3-Nd(2)-O(3)#2	109.33(13)	O(1)#4-Nd(2)-O(4)#2	120.31(12)	O(4)#2-Nd(2)-O(6)	166.82(12)

Complex **3**					
Dy(1)-O(12)#1	2.342(2)	Dy(1)-O(2)	2.457(2)	Dy(2)-O(9)	2.353(2)
Dy(1)-O(13)	2.363(3)	Dy(1)-O(1)	2.466(3)	Dy(2)-O(4)#2	2.376(2)
Dy(1)-O(3)#2	2.364(3)	Dy(1)-O(8)#3	2.614(2)	Dy(2)-O(6)#4	2.393(2)
Dy(1)-O(10)	2.388(2)	Dy(2)-O(11)	2.262(2)	Dy(2)-O(10)	2.584(2)
Dy(1)-O(5)	2.394(2)	Dy(2)-O(8)#3	2.305(2)	Dy(2)-O(5)#4	2.721(3)
Dy(1)-O(7)#3	2.447(2)	Dy(2)-O(2)#4	2.312(2)	Dy(2)-O(3)#2	2.744(4)
O(12)#1-Dy(1)-O(13)	70.13(9)	O(3)#2-Dy(1)-O(7)#3	117.67(10)	O(10)-Dy(1)-O(1)	77.50(8)
O(12)#1-Dy(1)-O(3)#2	146.39(10)	O(10)-Dy(1)-O(7)#3	89.82(9)	O(5)-Dy(1)-O(1)	119.00(9)
O(13)-Dy(1)-O(3)#2	140.14(10)	O(5)-Dy(1)-O(7)#3	85.63(10)	O(7)#3-Dy(1)-O(1)	153.97(12)
O(12)#1-Dy(1)-O(10)	143.34(8)	O(12)#1-Dy(1)-O(2)	76.49(8)	O(2)-Dy(1)-O(1)	51.71(7)
O(13)-Dy(1)-O(10)	74.15(9)	O(13)-Dy(1)-O(2)	109.04(9)	O(12)#1-Dy(1)-O(8)#3	121.80(8)
O(3)#2-Dy(1)-O(10)	70.08(10)	O(3)#2-Dy(1)-O(2)	78.22(10)	O(13)-Dy(1)-O(8)#3	111.34(9)
O(12)#1-Dy(1)-O(5)	75.48(8)	O(10)-Dy(1)-O(2)	124.04(7)	O(3)#2-Dy(1)-O(8)#3	68.12(9)
O(13)-Dy(1)-O(5)	144.73(9)	O(5)-Dy(1)-O(2)	69.13(8)	O(10)-Dy(1)-O(8)#3	64.88(7)
O(3)#2-Dy(1)-O(5)	75.04(9)	O(7)#3-Dy(1)-O(2)	146.14(9)	O(5)-Dy(1)-O(8)#3	80.43(8)
O(10)-Dy(1)-O(5)	137.65(8)	O(12)#1-Dy(1)-O(1)	101.26(11)	O(7)#3-Dy(1)-O(8)#3	50.27(8)
O(12)#1-Dy(1)-O(7)#3	75.52(8)	O(13)-Dy(1)-O(1)	76.09(11)	O(2)-Dy(1)-O(8)#3	139.37(8)
O(13)-Dy(1)-O(7)#3	78.62(11)	O(3)#2-Dy(1)-O(1)	79.52(12)	O(1)-Dy(1)-O(8)#3	136.55(9)
O(11)-Dy(2)-O(8)#3	80.38(9)	O(2)#4-Dy(2)-O(6)#4	95.36(8)	O(9)-Dy(2)-O(5)#4	112.28(9)
O(11)-Dy(2)-O(2)#4	84.21(8)	O(9)-Dy(2)-O(6)#4	81.71(9)	O(4)#2-Dy(2)-O(5)#4	132.40(8)
O(8)#3-Dy(2)-O(2)#4	163.27(8)	O(4)#2-Dy(2)-O(6)#4	164.39(10)	O(6)#4-Dy(2)-O(5)#4	49.62(7)
O(11)-Dy(2)-O(9)	157.12(9)	O(11)-Dy(2)-O(10)	144.95(8)	O(10)-Dy(2)-O(5)#4	124.47(7)
O(8)#3-Dy(2)-O(9)	118.29(8)	O(8)#3-Dy(2)-O(10)	66.47(8)	O(11)-Dy(2)-O(3)#2	95.74(9)
O(2)#4-Dy(2)-O(9)	78.25(8)	O(2)#4-Dy(2)-O(10)	129.87(7)	O(8)#3-Dy(2)-O(3)#2	66.60(8)
O(11)-Dy(2)-O(4)#2	77.32(10)	O(9)-Dy(2)-O(10)	51.88(7)	O(2)#4-Dy(2)-O(3)#2	121.81(8)
O(8)#3-Dy(2)-O(4)#2	107.24(9)	O(4)#2-Dy(2)-O(10)	101.19(8)	O(9)-Dy(2)-O(3)#2	81.44(9)
O(2)#4-Dy(2)-O(4)#2	75.38(9)	O(6)#4-Dy(2)-O(10)	74.86(7)	O(4)#2-Dy(2)-O(3)#2	48.55(8)
O(9)-Dy(2)-O(4)#2	84.08(10)	O(11)-Dy(2)-O(5)#4	72.62(8)	O(6)#4-Dy(2)-O(3)#2	134.48(8)
O(11)-Dy(2)-O(6)#4	114.76(9)	O(8)#3-Dy(2)-O(5)#4	103.12(8)	O(10)-Dy(2)-O(3)#2	61.52(7)
O(8)#3-Dy(2)-O(6)#4	85.29(9)	O(2)#4-Dy(2)-O(5)#4	65.73(7)	O(5)#4-Dy(2)-O(3)#2	166.07(9)

Symmetry operations: Complex **1**: #1 -x,y-1/2,-z+1/2; #2 -x+1,y+1/2,-z+1/2; #3 x,-y+1/2,z-1/2; #4 -x+1,-y,-z+1; #5 x,-y+1/2,z+1/2; #6 -x,-y+1, -z+1. Complex **2**: #1 x,-y+3/2,z+1/2; #2 -x,y+1/2,-z+1/2; #3 -x+1,-y+1,-z; #4 x,-y+3/2,z-1/2. Complex 3: #1 x,-y+3/2,z+1/2; #2 -x,y-1/2,-z+3/2; #3 -x+1,y+1/2,-z+3/2; #4 x,-y+3/2,z-1/2

In the coordination polymer **1**, the Pr^{3+} ions are interconnected through COO^- groups, forming 1D Pr–COO chains along the c-axis (Fig. 2). These 1D infinite chains may be viewed as supramolecular secondary building blocks, which are further cross-linked by the $–CH_2C_6H_4CH_2–$ spacers of pda^{2-} into a 3D network, exhibiting a compressed honeycomb shape with 1D open channels (Fig. 3). The one-end coordinated water molecules and guest water molecules are encapsulated in large channels. From the topological view, each Pr is a 6-connected node and each 1,4-pda^{2-} ligand is a 4-connected spacer. As a result, a unique trinodal 3D coordination network with (6,4)-connectivity is afforded (Fig. 4), with the Schläfli symbol of $(4^2.6^2.8^2)(4^3.6^3)_2(4^6.67.8^2)(4^8.6^7)$.

TGA results: Thermal stability of three complexes are studied by thermogravimetric analysis (TGA) under air atmosphere in 30-800 °C region at a heating rate of 10 °C h^{-1} (Fig. 5), they have also similar patterns. Therefore, only the patterns of **1** will be discussed as a representative. For **1**, the first weight losses of 5.08 % (calcd: 5.26 %) from 25 to 100 °C indicate the removing of lattice and coordination water molecules. The second weight loss is 59.06 % at 350-500 °C, assigning to the decomposition of 1,4-pda ligands (calcd. 58.57 %). The final stage can be considered as the decomposition of anhydrous composition to yield praseodymium oxide.

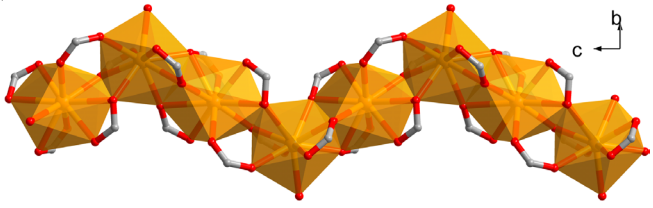

Fig. 2. View of 1D chain

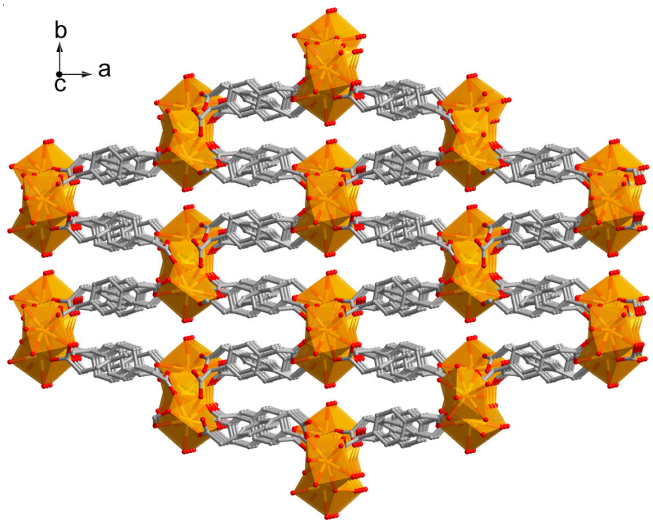

Fig. 3. Perspective view of complex **1** along the c axis, showing 3D network

Fluorescent properties: The room temperature solid-state fluorescence spectra of **1**, **2** and **3** are shown in Fig. 6. Upon excitation with λ_{ex} = 375 nm, free H_2pda give emissions at about 465 nm, which are probably due to the π–π* transition.

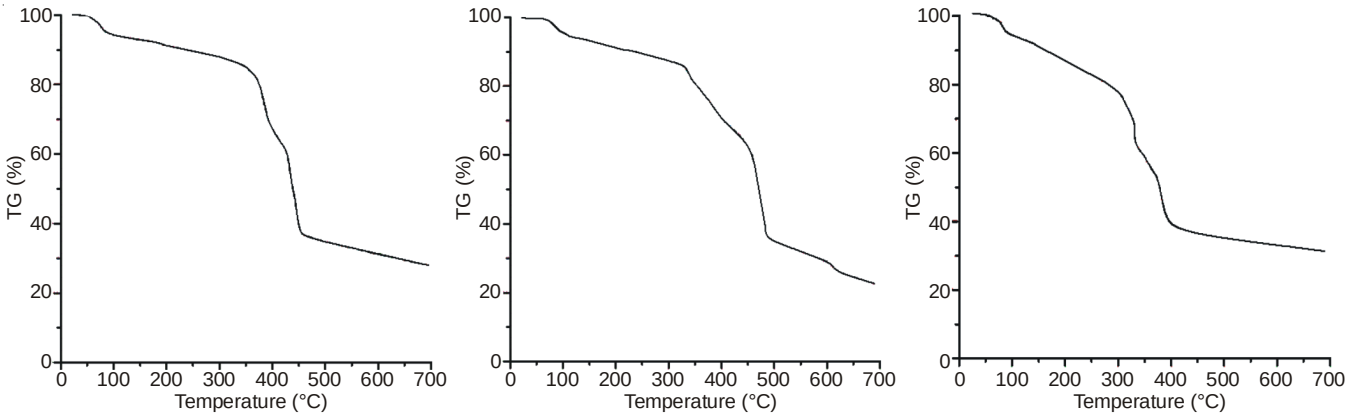

Fig. 5. TG curve for complex **1** (a), complex **2** (b) and complex **3** (c)

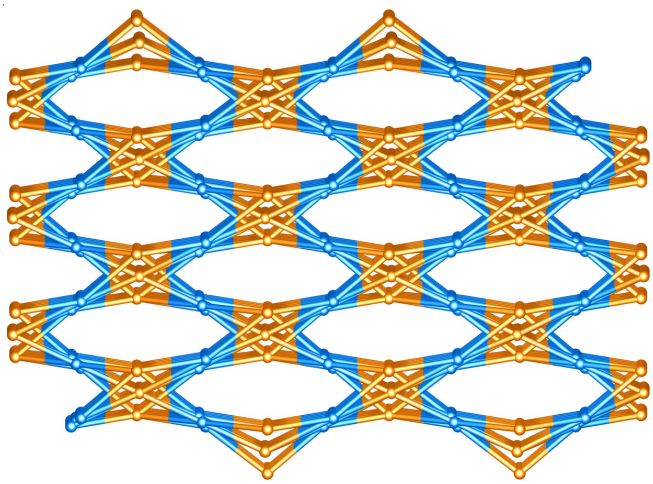

Fig. 4. Schematic view of the (4,6)-connected net in **1** (blue nodes for 4-connected pda^{2-} ligands and blue nodes for 6-connected Pr(III) centers)

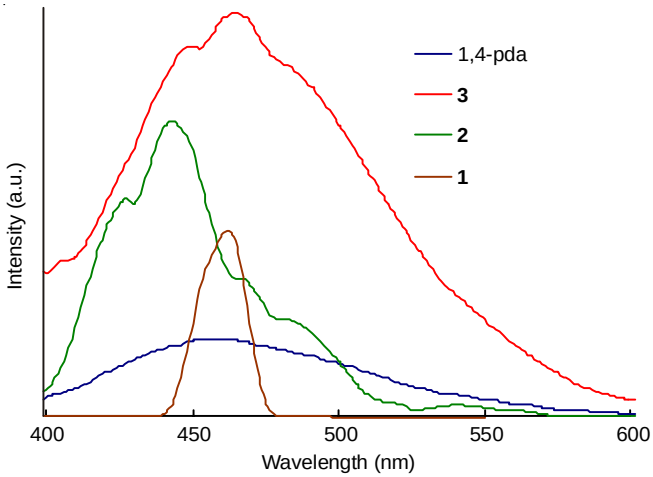

Fig. 6. Solid-state emission spectrum of **1**, **2**, **3** and 1,4-pda at room temperature

Three complexes **1**, **2** and **3** exhibit broad bands near about 464 nm, 446 nm and 469 nm. In comparison to the free 1,4-pda, the emission peaks of two complexes have a visible red or blue shift and its intensity is also increased, which can be attributed to intra ligand π–π* transition. From the above results, it is concluded that three complexes exhibit the characteristic emissions of 1,4-pda ligand, mainly because the energy matching between the triple state T_1 of 1,4-pda and the *f-f* electric transition ΔE_f of Ln^{3+}, which results in the efficient energy transfer.

ACKNOWLEDGEMENTS

This project was supported by the Natural Science Foundation of Yan'an University (YD2014-06), the Natural Scientific Research Foundation of Yan'an City Technology Division (2014ZC-3) and the Provincial College Students' Innovation and Entrepreneurship Training Program (1239).

REFERENCES

1. O.M. Yaghi, M. O'Keeffe, N.W. Ockwig, H.K. Chae, M. Eddaoudi and J. Kim, *Nature*, **423**, 705 (2003).
2. M. O'Keeffe and O.M. Yaghi, *Chem. Rev.*, **112**, 675 (2012).
3. M.W. Zhang, M. Bosch, T. Gentle III and H.C. Zhou, *CrystEngComm*, **16**, 4069 (2014).
4. Y. Zhao, D.S. Deng, L.F. Ma, B.M. Ji and L.Y. Wang, *Chem. Commun.*, **49**, 10299 (2013).
5. X.M. Wang, W.P. Wu, Y.H. Jiang, G.P. Yang and Z.P. Xi, *Wuji Huaxue Xuebao*, **30**, 192 (2014).
6. Y. Cui, Y. Yue, G. Qian and P. Chen, *Chem. Rev.*, **112**, 1126 (2012).
7. A. Morozan and F. Jaouen, *Energy Environ. Sci.*, **5**, 9269 (2012).
8. Y.P. Cai, X.X. Zhou, Z.Y. Zhou, S.Z. Zhu, P.K. Thallapally and J. Liu, *Inorg. Chem.*, **48**, 6341 (2009).
9. O.Z. Yesilel, G. Günay, C. Darcan, M.S. Soylu, S. Keskin and S.W. Ng, *CrystEngComm*, **14**, 2817 (2012).
10. L.J. Chen, X. Chen, Q.B. Hou, M.X. Yang and S. Lin, *Wuji Huaxue Xuebao*, **30**, 786 (2014).
11. H.Y. Deng, J.R. He, M. Pan, L. Li and C.Y. Su, *CrystEngComm*, **11**, 909 (2009).
12. Y.X. Ren, M.L. Zhang, D.S. Li, F. Fu, J.J. Wang, M. Du, X.Y. Hou and Y.P. Wu, *Inorg. Chem. Commun.*, **14**, 231 (2011).
13. C.Y. Wang, X.S. Wu and X. Li, *Wuji Huaxue Xuebao*, **24**, 781 (2008).
14. J. Wang and X.Q. Zhao, *Chinese J. Struct. Chem.*, **33**, 7 (2014).
15. J. Wang, Y.H. Zhang and M.L. Tong, *Chem. Commun. (Camb.)*, 3166 (2006).
16. L. Pan, K.M. Adams, H.E. Hernandez, X. Wang, C. Zheng, Y. Hattori and K. Kaneko, *J. Am. Chem. Soc.*, **125**, 3062 (2003).
17. Y.W. Ren, J.X. Liang, J.X. Lu, B.W. Cai, D.B. Shi, C.R. Qi, H.F. Jiang, J. Chen and D. Zheng, *Eur. J. Inorg. Chem.*, **2011**, 4369 (2011).
18. G.M. Sheldrick, SADABS, A Program for Empirical Absorption Correction of Area Detector Data, University of Göttingen, Germany (1997).
19. G.M. Sheldrick, SHELXS-97, Program for the Solution of Crystal Structures, University of Göttingen, Germany (1997).
20. G.M. Sheldrick, SHELXL-97, Program for the Refinement of Crystal Structures, University of Göttingen, Germany (1997).